Jpn. J. Cancer Res. **91**, 845–852, August 2000

In vitro Plasma Protein Binding and Cellular Uptake of ATX-S10(Na), a Hydrophilic Chlorin Photosensitizer

Masahiko Mori,[1,6] Toyoshi Kuroda,[1] Akira Obana,[2] Isao Sakata,[3] Toru Hirano,[4] Susumu Nakajima,[5] Muneo Hikida[1] and Toshio Kumagai[1]

[1]Medical Research Laboratories, Wyeth Lederle Japan, Ltd., 1-6-34 Kashiwa-cho, Shiki 353-8511, [2]Department of Ophthalmology, Osaka City University Medical School, 1-4-3 Asahimachi, Abeno-ku, Osaka 545-8585, [3]Photochemical Co., Ltd., 5301 Haga, Okayama 701-1221, [4]Photon Medical Research Center, Hamamatsu University School of Medicine, 3600 Handa-cho, Hamamatsu 431-3192 and [5]Division of Surgical Operation, Asahikawa Medical College, 1-1-1 Midorigaoka-higashi-2-jo, Asahikawa 078-8510

ATX-S10(Na), a hydrophilic chlorin photosensitizer having an absorption maximum at 670 nm, is a candidate second-generation photosensitizer for photodynamic therapy (PDT) for cancer treatment. In this study, we examined plasma protein binding, cellular uptake and subcellular targets of ATX-S10(Na) *in vitro*. Protein binding ratios of 50 μg/ml ATX-S10(Na) in rat, dog and human plasma were 73.0%, 87.2% and 97.7%, respectively. Gel filtration chromatography revealed that 1 mg/ml ATX-S10(Na) bound mainly to high-density lipoprotein (HDL) and serum albumin at the protein concentration of 0.4%, with binding ratios of 46% and 36%, respectively. The free form of ATX-S10(Na) was mostly incorporated into T.Tn cells, and its cellular uptake was partially but significantly inhibited by endocytosis inhibitors such as phenylarsine oxide, chloroquine, monensin and phenylglyoxal, and by chilling the cells to 4°C. However, ouabain, harmaline, sodium cyanide, probenecid and aspartic acid did not influence the uptake of ATX-S10(Na), suggesting that cellular uptake of ATX-S10(Na) was not related to sodium-potassium pump activity, sodium-dependent transporter activity, mitochondrial oxidative respiration, organic anion transporter activity or aspartic acid transporter activity. By fluorescence microscopy, lysosomal localization of ATX-S10(Na) was observed in T.Tn cells. However, electron microscopic observation revealed that many subcellular organelles such as mitochondria, endoplasmic reticulum, ribosomes, Golgi complex and plasma membrane were damaged by PDT using 25 μg/ml ATX-S10(Na) soon after laser irradiation at 50 J/cm^2, and tumor necrosis was rapidly induced. This result indicated that ATX-S10(Na) was widely distributed within the cell.

Key words: Photodynamic therapy — ATX-S10(Na) — Protein binding — Cellular uptake — Subcellular localization

Photodynamic therapy (PDT) has been developed as a treatment for superficial cancer with laser irradiation following systemic administration of a tumor-localizing photosensitized agent. Although porfimer sodium is the only commercially available photosensitizer, patients are obliged to avoid the sun for several weeks after PDT in order to avoid developing hyperphotosensitivity of the skin. ATX-S10(Na), which has been developed as a second-generation photosensitizer, shows potent anti-tumor activity in combination with a 670-nm diode laser, and is rapidly eliminated from the body so that hyperphotosensitivity is expected to be reduced.[1–3)]

The effectiveness of PDT is based on the selective localization of photosensitizers in target tissues. Some photosensitizers such as porfimer sodium bind to low-density lipoprotein (LDL), and the LDL receptor-mediated endocytic pathway is a well-known mechanism of tumor cell-specific accumulation of photosensitizers.[4)] Although there are some reports suggesting tumor-specific accumulation of ATX-S10(Na),[1, 5)] the mechanisms of tissue distribution and cellular uptake of ATX-S10(Na) remain unclear. In the present study, we investigated the plasma protein binding, cellular uptake and subcellular targets of ATX-S10(Na) *in vitro*.

MATERIALS AND METHODS

Photosensitizer ATX-S10(Na), 13,17-bis(1-carboxypropionyl)carbamoylethyl-8-ethenyl-2-hydroxy-3-hydroxyiminoethylidene-2,7,12,18-tetramethylporphyrin sodium salt, was synthesized by Toyo Hakka Kogyo Co., Ltd. (Okayama). The chemical structure of ATX-S10(Na) is shown in Fig. 1. ATX-S10(Na) was dissolved in phosphate-buffered saline (PBS) and diluted with culture medium at appropriate concentrations.

[6] To whom correspondence should be addressed.
E-mail: morim@labs.wyeth.com

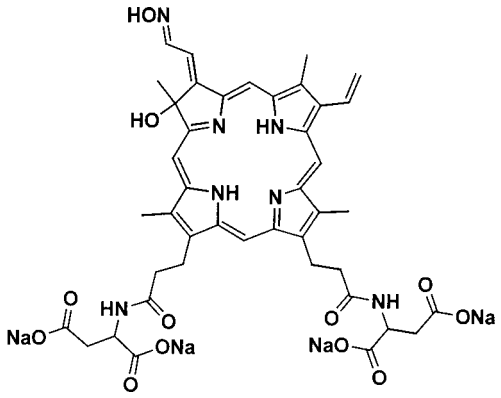

Fig. 1. Chemical structure of ATX-S10(Na).

Chemicals Phenylarsine oxide, chloroquine, monensin, phenylglyoxal, harmaline and probenecid were purchased from Sigma-Aldrich Japan K. K. (Tokyo). Ouabain, sodium cyanide, aspartic acid, glycine, alanine, histidine and other reagents were obtained from Wako Pure Chemical Industries, Ltd. (Osaka).

Laser units A diode laser (LD670-05, Hamamatsu Photonics K. K., Hamamatsu) was used as a light source for exciting ATX-S10(Na). The diode laser is a continuous-wave laser operating at 670-nm wavelength.

Tumor T.Tn, human esophageal cancer, was purchased from Human Science Research Resource Bank (Osaka). T.Tn cells were grown in Dulbecco's modified Eagle's medium supplemented with 10% fetal calf serum (FCS) and antibiotics (100 units/ml benzylpenicillin and 100 μg/ml streptomycin) under a humidified atmosphere containing 5% CO_2 at 37°C.

Plasma and human plasma proteins Rat, mouse, dog and human plasma were prepared in our laboratory. Human plasma proteins (serum albumin, transferrin, haptoglobin, fibrinogen type I, fibrinogen type III, high-density lipoprotein (HDL) and LDL) were purchased from Sigma-Aldrich Japan K. K.

Measurement of protein binding of ATX-S10(Na) *in vitro* Rat, dog or human plasma was incubated with 50 μg/ml ATX-S10(Na) for 20 min at 37°C. After centrifugation at 235 000*g* for 16 h at 4°C, 100 μl of the supernatant was mixed with 25 μl of 40 m*M* dithiothreitol, 25 μl of 10% trichloroacetic acid and 300 μl of methanol. The samples were sonicated for 10 min, allowed to stand for 1 h and centrifuged at 1500*g* for 10 min at 4°C. The concentration of ATX-S10(Na) in the supernatant was determined by high-performance liquid chromatography (HPLC). The HPLC system consisted of a Waters LC module 1 (Waters, Tokyo) with an Inertsil ODS-2 column (5 μm octadecyl silica (ODS), 250 mm×4.6 mm i.d.; GL Sciences Inc., Tokyo). ATX-S10(Na) was detected with a Waters 470 Scanning Fluorescence Detector at the wavelength of 667 nm with excitation at 413 nm. The mobile phase was 60% water, 10% acetic acid and 30% acetonitrile, and the flow rate was 1.1 ml/min. The plasma protein binding ratio of ATX-S10(Na) was calculated by means of the following equation: Binding ratio (%)=$(C_p-C_s)/C_p\times100$, where C_p and C_s indicate the concentrations of ATX-S10(Na) in the plasma and in the supernatant, respectively.

Agarose gel electrophoresis One microliter of human plasma and 1 μl of 500 μg/ml ATX-S10(Na) were mixed and applied to the agarose gel plate of a TAITAN GEL High Resolution Protein System (Helena Laboratories, Beaumont, TX) and electrophoresed at 250 V for 15 min. After electrophoresis, the agarose gel was cut into 5-mm slices in the direction of electrophoresis. Each gel piece was put into a glass tube with 1 ml of water and homogenized with a Physcotron (NS-310E, Microtec Co., Ltd., Funabashi). After centrifugation of the homogenate at 1500*g* for 5 min, the concentration of ATX-S10(Na) in the supernatant was determined with a fluorescence spectrophotometer (F-3000, Hitachi, Tokyo) at the excitation wavelength of 413 nm and the fluorescence wavelength of 667 nm. As control samples, 1 μl of 500 μg/ml ATX-S10(Na) and 1 μl of human plasma were also analyzed by the same procedure.

Gel filtration chromatography A mixture of 20% mouse serum and 1 mg/ml ATX-S10(Na) was applied to a TSK-GEL G3000SW gel filtration column (300 mm×7.5 mm i.d.; Tosoh, Tokyo). The HPLC system consisted of a Waters 600S controller, 626 pump, 717 plus autosampler and 490E detector (Waters). Protein and ATX-S10(Na) were detected as absorbance at wavelengths of 280 and 395 nm, respectively. The mobile phase was 50 m*M* phosphate buffer (pH 7.0) containing 0.05% NaN_3. A mixture of 0.4% of each human plasma protein (serum albumin, transferrin, haptoglobin, fibrinogen type I, fibrinogen type III, HDL and LDL) and 1 mg/ml ATX-S10(Na) was also analyzed by the same procedure. Binding ratios of ATX-S10(Na) to human plasma proteins were calculated by means of the following equation: Binding ratio (%)=(Peak area of protein-bound ATX-S10(Na))/(Total peak area of ATX-S10(Na))×100.

Measurement of cellularly incorporated ATX-S10(Na) T.Tn cells were incubated with 50 μg/ml ATX-S10(Na) and 10% FCS for a designated time in the presence or absence of endocytosis inhibitors, such as phenylarsine oxide,[6,7] chloroquine,[8,9] monensin[10] and phenylglyoxal,[11–13] or at the low incubation temperature at 4°C.[14,15] Cells were collected by trypsinization, then 0.5% Nonidet P-40 solution was added to adjust the cell concentration to 10^6 cells/ml. Cells were homogenized by vigorous mixing and centrifuged at 1500*g* for 10 min. ATX-S10(Na) concentration in the supernatant was determined with a fluorescence spectrophotometer at the excitation wave-

length of 413 nm and fluorescence wavelength of 667 nm. Protein concentration in the supernatant was measured with BCA Protein Assay (Pierce, Rockford, IL). The effects of ouabain, harmaline, sodium cyanide, probenecid and amino acids on cellular uptake of ATX-S10(Na) were also investigated by using the same procedure.

Fluorescence microscopy T.Tn cells were grown on coverslips and incubated with 50 μg/ml ATX-S10(Na) for 24 h at 37°C. The cells were washed twice with PBS and stained with 0.1 μM Nile Blue A,[16] a lysosomal dye, for 2 min at room temperature. They were further washed with PBS, and the fluorescence of ATX-S10(Na) or Nile Blue A was observed with a fluorescence microscope (XF-EFD, Nikon, Tokyo) equipped with a V exciter filter or G exciter filter, respectively, which blocks the fluorescence of the other component.

Analysis of subcellular targets of PDT by transmission electron microscopy (TEM) T.Tn cells were grown in an 8-well chamber slide and incubated with 25 μg/ml ATX-S10(Na) at 37°C for 24 h. The cells were washed with PBS, then irradiated with the 670-nm diode laser at 50 J/cm^2 from the underside of the chamber slide. Immediately after and at 15, 30, 45 min, 1, 2 and 4 h after laser irradiation, cells were fixed with 2.5% glutaraldehyde, post-fixed with 1% osmium tetroxide solution, dehydrated in serial ethanol and embedded in Acrafilm (Nisshin EM Co., Ltd., Tokyo). The samples were thinly cut, stained with uranyl acetate and lead citrate, and examined with a Hitachi H-7000 electron microscope.

RESULTS

***In vitro* plasma protein binding of ATX-S10(Na)** When ATX-S10(Na) at a final concentration of 50 μg/ml was added to rat, dog and human plasma *in vitro*, large amounts of ATX-S10(Na) bound to plasma proteins with the binding ratios of 73.0%, 87.2% and 97.7%, respectively (Table I). In order to separate the ATX-S10(Na)-binding proteins, agarose gel electrophoresis and gel filtration chromatography were performed. Agarose gel electrophoresis showed the presence of protein-bound ATX-S10(Na) in the albumin fraction and α_1-globulin fraction, but not in the β- and γ-globulin fractions (Fig. 2). By gel

Table I. Protein Binding Ratio of ATX-S10(Na) in Rat, Dog and Human Plasma

Species	Binding ratio (%, mean±SD, n=3)
Rat	73.0±1.7
Dog	87.2±4.9
Human	97.7±1.6

ATX-S10(Na) concentration: 50 μg/ml.

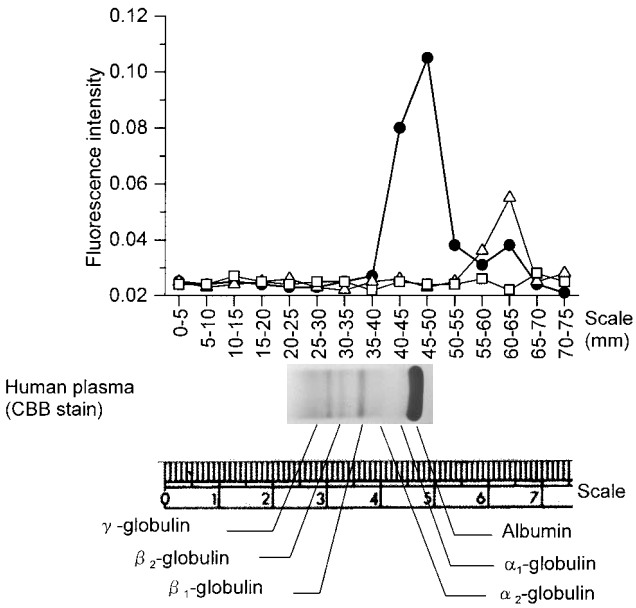

Fig. 2. Agarose gel electrophoresis of a mixture of human plasma and ATX-S10(Na). Mixture of 1 μl of human plasma and 1 μl of 500 μg/ml ATX-S10(Na) was applied to agarose gel and electrophoresed at 250 V for 15 min. The agarose gel was cut into 5-mm slices. After homogenization of each gel slice, the fluorescence intensity of ATX-S10(Na) in the homogenate was determined with a fluorescence spectrophotometer (ex. 413 nm, em. 667 nm). ● ATX-S10(Na)+human plasma, △ ATX-S10(Na), □ human plasma. CBB: Coomassie Brilliant Blue.

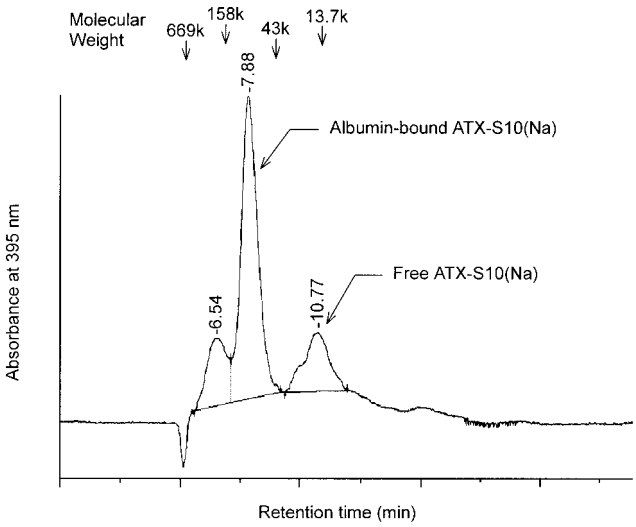

Fig. 3. Gel filtration chromatography of mouse serum and ATX-S10(Na). Mouse serum (final concentration 20%) and ATX-S10(Na) (final 1 mg/ml) were mixed and applied to an HPLC gel filtration column as described in "Materials and Methods." ATX-S10(Na) was detected in terms of absorbance at 395 nm.

Table II. Binding Ratio of ATX-S10(Na) to Human Plasma Proteins

Protein	Binding ratio (%)
High-density lipoprotein	46
Serum albumin	36
Fibrinogen type I	28
Fibrinogen type III	24
Transferrin	18
Haptoglobin	12
Low-density lipoprotein	10

Protein concentration: 0.4%.
ATX-S10(Na) concentration: 1 mg/ml.

Table III. Cellular Uptake of ATX-S10(Na) in the Presence of Human Serum Albumin (HSA), High-density Lipoprotein (HDL) and Low-density Lipoprotein (LDL) in T.Tn Cells

Protein	Protein concentration (mg/ml)	ATX-S10(Na) uptake[a] (% of control)
—	0	100.0
HSA	5	16.7±1.3
	10	8.4±0.4
HDL	0.1	94.2±4.7
	0.3	71.6±8.3
	1	23.2±1.1
LDL	0.1	100.0±8.3
	0.3	103.7±3.9
	1	109.5±13.2

a) Data represent mean±SD (n=3).
ATX-S10(Na) concentration: 50 μg/ml. Incubation time: 24 h.

filtration chromatography, peaks of ATX-S10(Na) were detected at retention times of 6.25, 7.88 and 10.77 min (Fig. 3). Peaks of ATX-S10(Na) at 7.88 and 10.77 min were thought to be due to albumin-bound ATX-S10(Na) and free ATX-S10(Na), respectively. A peak at 6.45 min corresponded to the molecular weight of 300–400 k. To identify the ATX-S10(Na)-binding proteins having a molecular weight of 300–400 k, we used purified plasma proteins as standards [haptoglobin (100–400 k), fibrinogen (340 k) and HDL (200–400 k)]. In addition, we also used transferrin, LDL and serum albumin, which have been reported to associate with other photosensitizers.[4, 17, 18] When 0.4% of each plasma protein and 1 mg/ml ATX-S10(Na) were mixed and analyzed by gel filtration chromatography, peaks of protein-bound ATX-S10(Na) were detected with all plasma proteins tested, and the binding ratios were HDL (46%)>serum albumin (36%)>fibrinogen type I (28%)>fibrinogen type III (24%)>transferrin (18%)>haptoglobin (12%)>LDL (10%) (Table II). In addition, when T.Tn cells were incubated with 50 μg/ml ATX-S10(Na) for 24 h in the presence of HDL, serum albumin and LDL, cellular uptake of ATX-S10(Na) was inhibited by HDL and serum albumin, but not by LDL

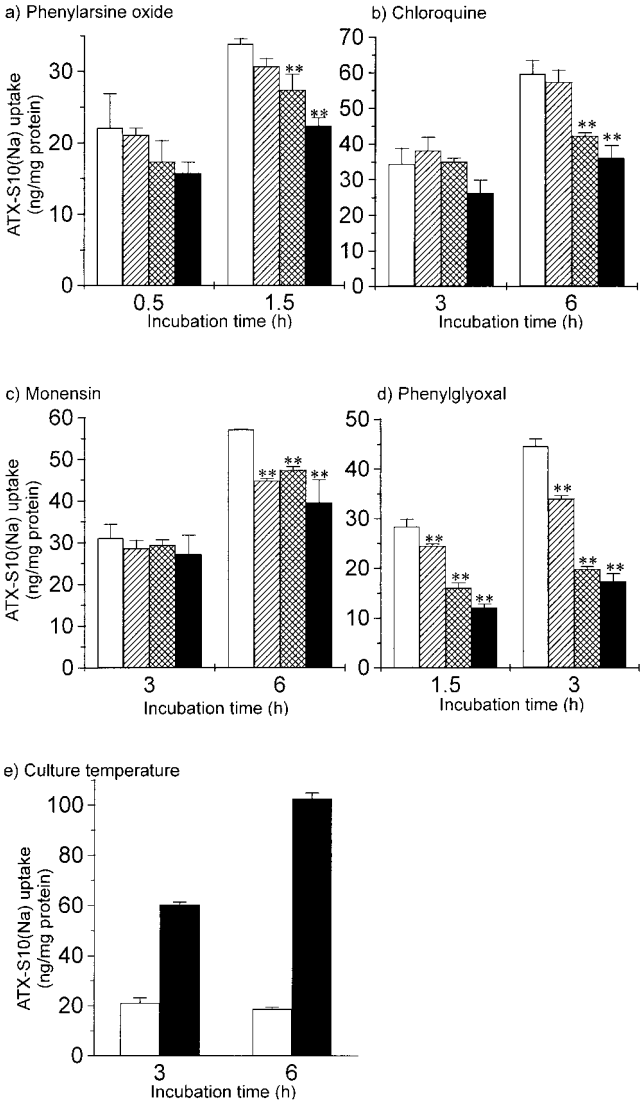

Fig. 4. Effects of endocytosis inhibitors and low temperature on cellular uptake of ATX-S10(Na) in T.Tn cells. T.Tn cells were incubated with 50 μg/ml ATX-S10(Na) and 10% FCS in the presence or absence of endocytosis inhibitors (phenylarsine oxide, chloroquine, monensin and phenylglyoxal), or at 4°C. Cellularly incorporated ATX-S10(Na) was measured with a fluorescence spectrophotometer (ex. 413 nm, em. 667 nm). Data represent mean±SD (n=3). ** Significantly different from the control group (no endocytosis inhibitors) at P<0.01 (Dunnett's multiple comparison test). a) □ 0 μM, ▨ 2.5 μM, ▩ 5 μM, ■ 10 μM; b) □ 0 μM, ▨ 100 μM, ▩ 200 μM, ■ 400 μM; c) □ 0 μM, ▨ 12.5 μM, ▩ 25 μM, ■ 50 μM; d) □ 0 mM, ▨ 0.5 mM, ▩ 1 mM, ■ 2 mM; e) □ 4°C, ■ 37°C.

Table IV. Effects of Metabolic Inhibitors, Organic Anion, and Amino Acids on Cellular Uptake of ATX-S10(Na)

Compound	Concentration (m*M*)	ATX-S10(Na) uptake[a] (% of control)
—	0	100.0
Ouabain	0.03	97.2±6.1
	0.1	98.1±8.3
	0.3	89.2±12.7
	1	97.3±0.9
Harmaline	0.03	99.1±6.3
	0.1	108.2±3.9
	0.3	116.2±8.1
	1	110.4±3.5
Sodium cyanide	0.03	98.6±3.5
	0.1	98.3±4.1
	0.3	95.3±2.1
	1	94.8±1.6
Probenecid	0.03	112.3±3.0
	0.1	105.5±7.4
	0.3	113.1±15.1
	1	115.7±9.8
Aspartic acid	0.1	94.4±4.5
	0.5	100.9±1.8
	1	95.3±4.7
	5	92.0±1.3

a) Data represent mean±SD (n=3).
ATX-S10(Na) concentration: 50 μg/ml.
Incubation time: 3 h.

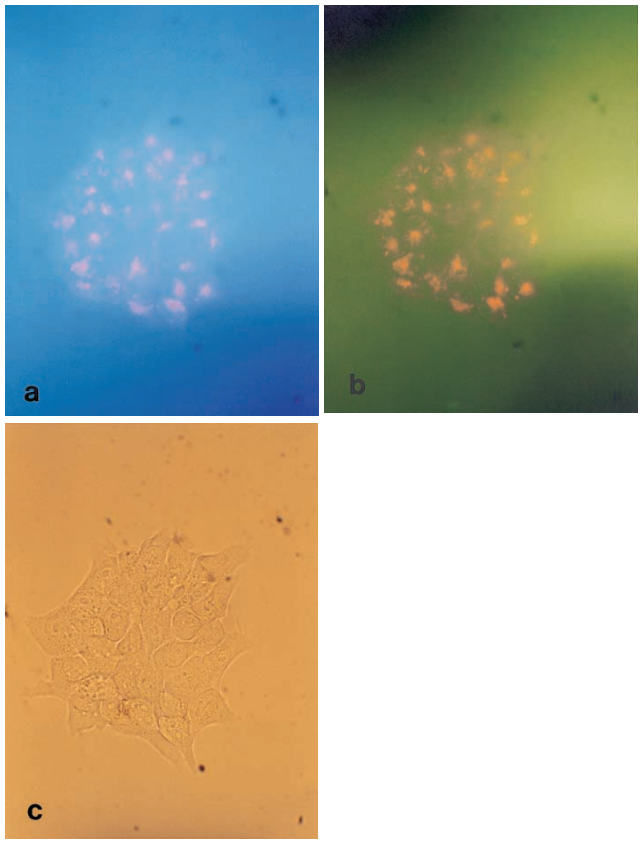

Fig. 5. Lysosomal localization of ATX-S10(Na). T.Tn cells were incubated with 50 μg/ml ATX-S10(Na) for 24 h and sequentially stained with Nile Blue A. a) ATX-S10(Na) and b) Nile Blue A were detected by fluorescence microscopy using a V exciter filter and a G exciter filter, respectively. c) A light micrograph of the T.Tn cells.

(Table III), suggesting that the free fraction of ATX-S10(Na) was incorporated into cells.

Cellular uptake mechanism of ATX-S10(Na) It has been reported that some photosensitizers are incorporated into cells via an endocytic pathway or by simple diffusion.[4, 15] As we hypothesized that ATX-S10(Na) would be taken up by endocytosis because of its hydrophilic character, we examined the effect of endocytosis inhibitors and low culture temperature on cellular uptake of ATX-S10(Na). When T.Tn cells were incubated with 50 μg/ml ATX-S10(Na) in the presence of endocytosis inhibitors at 37°C or incubated with it at 4°C, the cellular uptake of ATX-S10(Na) was partially but significantly inhibited by all endocytosis inhibitors tested and also by chilling the cells to 4°C, indicating that endocytosis is one of the uptake mechanisms of ATX-S10(Na) (Fig. 4). Although in the case of incubation at 4°C, the amount of incorporated ATX-S10(Na) did not increase with time, 20 ng/mg protein of ATX-S10(Na) was detected in the cells. Therefore, it is considered that ATX-S10(Na) can bind to the cell membrane.

We next examined whether a transporter-mediated mechanism contributed to the cellular uptake of ATX-S10(Na), using ouabain (Na^+-K^+-ATPase inhibitor), harmaline (Na^+-dependent transporter inhibitor), sodium cyanide (mitochondrial oxidative metabolism inhibitor), probenecid (organic anion transporter inhibitor) and aspartic acid (as ATX-S10(Na) is an organic anion having aspartic acid residues). As shown in Table IV, none of the inhibitors tested inhibited cellular uptake of ATX-S10(Na).

Subcellular localization of ATX-S10(Na) In order to examine the subcellular distribution of ATX-S10(Na), we compared the fluorescence pattern of ATX-S10(Na) with that of Nile Blue A, a dye staining lysosomes. When T.Tn cells were double-stained with ATX-S10(Na) and Nile Blue A, the fluorescence pattern of ATX-S10(Na) corresponded with that of Nile Blue A (Fig. 5). We also compared the fluorescence pattern of ATX-S10(Na) with that of Rhodamine 123, a dye for mitochondria, but the fluorescence patterns were different (data not shown).

Cellular destruction by *in vitro* PDT Damage to subcellular organelles after *in vitro* PDT was investigated by

Table V. Ultrastructural Changes of Subcellular Organelles after PDT *in vitro*

Findings	Time after laser irradiation (min)						
	0	15	30	45	60	120	240
Formation of cytoplasmic vacuoles	−	+	+	+	−	−	−
Disaggregation of polyribosomes	+	+	+	+	−	−	−
Degranulation of rough endoplasmic reticulum	−	−	+	+	−	−	−
Dissolution of membranes of Golgi complex and endoplasmic reticulum	−	+	+	+	−	−	−
Vesiculation of endoplasmic reticulum/increase in cytoplasmic vesicles	−	−	−	+	−	−	−
Mitochondrial swelling	+	−	+	+	−	−	−
Condensation of mitochondria with longitudinally oriented cristae	−	+	+	+	−	−	−
Decrease in surface processes	+	−	−	−	−	−	−
Formation of bleb-like surface processes	−	−	−	+	−	−	−
Accumulation of microfilaments in marginal cytoplasm	−	−	−	+	−	−	−
Swollen and disrupted cytoplasmic organelles	−	−	−	−	+	+	+
Karyolysis	−	−	−	−	+	+	+

−, not remarkable; +, present.

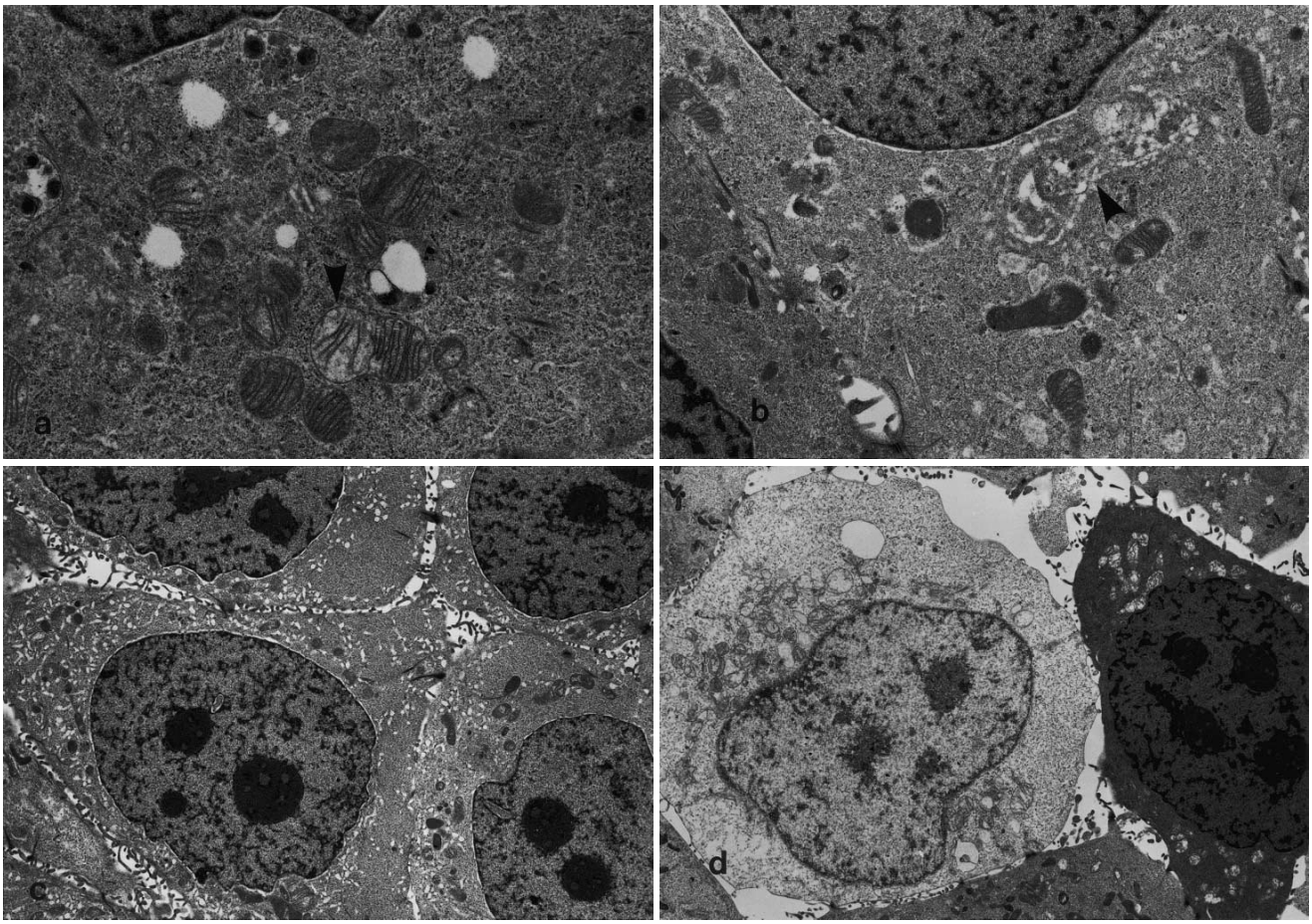

Fig. 6. Electron micrographs of T.Tn cells after PDT using ATX-S10(Na). a) Immediately after PDT, mitochondrial swelling is already apparent (arrowhead). b) 15 min after PDT, dissolution of the membrane of the Golgi complex is induced (arrowhead). c) 45 min after PDT, many cytoplasmic vesicles are observed. d) 1 h after PDT, most cytoplasmic organelles and nuclei are disrupted.

TEM. After 24-h exposure of T.Tn cells to 25 μg/ml ATX-S10(Na), the cells were irradiated with a diode laser at 50 J/cm^2 and fixed at the designated time. As shown in Table V, within 45 min after laser irradiation, many organelles such as mitochondria (Fig. 6a), endoplasmic reticulum, ribosomes, Golgi complex (Fig. 6b) and plasma membrane had degenerated, and 1 h after PDT, disruption of cytoplasm (Fig. 6c) and nuclei, followed by cell-death (Fig. 6d), was observed.

DISCUSSION

The effect of PDT is based on the selective localization of photosensitizers in target tissues. Mazière *et al*. have reported that photosensitizers such as porfimer sodium and benzoporphyrin derivative bind to LDL and are cellularly incorporated via the LDL receptor-mediated endocytic pathway.[4] In fact, LDL receptors are found in tumor tissues more than in some normal tissues,[19–21] explaining the selective localization of LDL-bound photosensitizer in tumor tissues. On the other hand, N-aspartyl chlorin-e6 (NPe6), which is a hydrophilic chlorin photosensitizer, mainly binds to albumin (80%) and HDL (19%), but only 1% of the sensitizer binds to LDL.[17] Therefore, the cellular uptake mechanism of NPe6 can not be explained in terms of the LDL receptor-mediated pathway and its mechanism of tumor-accumulation remains unclear.

Several studies have demonstrated that ATX-S10(Na) is selectively accumulated in tumor tissues in experimental animals.[1, 22] To clarify the cellular uptake mechanism of ATX-S10(Na), we firstly investigated plasma protein binding of ATX-S10(Na). As shown in Table I, most of the ATX-S10(Na) bound to plasma proteins *in vitro*. When 5 mg/kg of ATX-S10(Na), which is an effective dose in tumor-bearing mice,[3] is intravenously administered in experimental animals, the maximal plasma concentration of ATX-S10(Na) is about 100 μg/ml (unpublished results). Within 15 min, the concentration decreases to about 50 μg/ml owing to tissue-distribution and excretion. Therefore, it is suggested that, after systemic administration of ATX-S10(Na) at an effective dose, most of the ATX-S10(Na) in blood may bind to plasma proteins, especially to HDL and serum albumin *in vivo*.

When protein-bound ATX-S10(Na) reaches tumor tissues, a part of the ATX-S10(Na) may be released as the free form and be incorporated into cells partly by endocytosis. Other possible uptake mechanisms of ATX-S10(Na), such as a transporter-mediated pathway, remain to be fully investigated. As shown in Table IV, however, ATX-S10(Na) uptake was not related to sodium-potassium pump activity, sodium-dependent transporter activity, mitochondrial oxidative respiration, organic anion transporter activity or aspartic acid transporter activity. The finding that some ATX-S10(Na) was detected in cells chilled to 4°C suggests that ATX-S10(Na) can associate with cell-surface proteins, such as a transporter, or lipids in the plasma membrane. The low affinity of ATX-S10(Na) for LDL indicates that the LDL receptor-mediated endocytic pathway may play only a minor role in uptake of ATX-S10(Na). Whether ATX-S10(Na) is incorporated by receptor-mediated endocytosis or by fluid phase endocytosis (pinocytosis), what kinds of transporters, if any, are concerned with ATX-S10(Na) uptake, and its tumor-localizing mechanism remain as problems for further investigations.

The subcellular distribution pattern of fluorescence of ATX-S10(Na) coincided with that of Nile Blue A, suggesting that ATX-S10(Na) is mainly accumulated in lysosomes. This result is consistent with the idea that ATX-S10(Na) is incorporated partly by endocytosis. However, electron microscopic observation of tumor cells after *in-vitro* PDT using ATX-S10(Na) revealed that many organelles such as mitochondria, Golgi complex, endoplasmic reticulum, ribosomes and plasma membrane were also affected within 45 min after PDT (Table V). These results suggest that ATX-S10(Na) may be mainly localized in lysosomes, but is also widely distributed to many organelles within the cell. NPe6 and chloro-aluminum sulfonated phthalocyanine have been reported to be incorporated by endocytosis and localized in only lysosomes.[15] On the other hand, porfimer sodium is mainly localized in mitochondria, because it can enter cells not only by endocytosis, but also by simple diffusion across the plasma membrane.[15] Such a difference in cellular uptake is thought to be due to the difference in the chemical properties of the sensitizers. Hydrophilic sensitizers such as NPe6 can not diffuse across the cell membrane, whereas lipophilic sensitizers such as porfimer sodium can diffuse across the membrane. The chemical structure and properties of ATX-S10(Na) are similar to those of NPe6. However, the mode of cellular destruction by ATX-S10(Na) is different from that of NPe6, which primarily destroys only lysosomes and has no effect on other organelles even 2 h after PDT.[23] We speculate that there may be some ATX-S10(Na)-specific distribution mechanisms in the cell.

In conclusion, ATX-S10(Na) mainly bound to serum albumin and HDL in plasma, and the free form of ATX-S10(Na) was incorporated into cells partly via the endocytic pathway. Cellularly incorporated ATX-S10(Na) was distributed not only to lysosomes, but also to many organelles, so that tumor destruction was rapidly induced *in vitro*.

ACKNOWLEDGMENTS

We wish to express our appreciation to Professor T. Irimura at the University of Tokyo for his review of the manuscript.

(Received February 17, 2000/Revised June 5, 2000/Accepted June 8, 2000)

REFERENCES

1) Nakajima, S., Sakata, I., Takemura, T. and Hayashi, H. Photo-chlorin (ATX-S10) as a new photosensitizer for PDT. *In* "Frontiers of Photobiology," ed. A. Shima, pp. 493–496 (1993). Elsevier Science, Amsterdam.
2) Nakajima, S., Sakata, I., Hirano, T. and Takemura, T. Therapeutic effect of interstitial photodynamic therapy using ATX-S10(Na) and a diode laser on radio-resistant SCCVII tumors of C3H/He mice. *Anticancer Drugs*, **9**, 539–543 (1998).
3) Mori, M., Sakata, I., Hirano, T., Obana, A., Nakajima, S., Hikida, M. and Kumagai, T. Photodynamic therapy for experimental tumors using ATX-S10(Na), a hydrophilic chlorin photosensitizer, and diode laser. *Jpn. J. Cancer Res.*, **91,** 753–759 (2000).
4) Mazière, J. C., Morliere, P. and Santus, R. The role of the low density lipoprotein receptor pathway in the delivery of lipophilic photosensitizers in the photodynamic therapy of tumors. *J. Photochem. Photobiol. B*, **8**, 351–360 (1991).
5) Tajiri, H., Yokoyama, K., Boku, N., Ohtsu, A., Fujii, T., Yoshida, S., Sato, T., Hakamata, K., Hayashi, K. and Sakata, I. Fluorescent diagnosis of experimental gastric cancer using a tumor-localizing photosensitizer. *Cancer Lett.*, **111**, 215–220 (1997).
6) Gibson, A. E., Noel, R. A., Herlihy, J. T. and Ward, W. F. Phenylarsine oxide inhibition of endocytosis: effect on asialofetuin internalization. *Am. J. Physiol.*, **257**, C182–C184 (1989).
7) Frost, S. C., Lane, M. D. and Gibbs, E. M. Effect of phenylarsine oxide on fluid phase endocytosis: further evidence for activation of the glucose transporter. *J. Cell. Physiol.*, **141**, 467–474 (1989).
8) Leppla, S. H., Dorland, R. B. and Middlebrook, J. L. Inhibition of diphtheria toxin degradation and cytotoxic action by chloroquine. *J. Biol. Chem.*, **255**, 2247–2250 (1980).
9) Sandvig, K., Olsnes, S. and Pihl, A. Inhibitory effect of ammonium chloride and chloroquine in the entry of the toxic lectin modeccin into HeLa cells. *Biochem. Biophys. Res. Commun.*, **90**, 648–655 (1979).
10) Marnell, M. H., Stookey, M. and Draper, R. K. Monensin blocks the transport of diphtheria toxin to the cell cytoplasm. *J. Cell Biol.*, **93**, 57–62 (1982).
11) van Schaik, M. L., Weening, R. S. and Roos, D. Phenylglyoxal is not a selective inhibitor of phagocytosis. *J. Cell Sci.*, **38**, 331–343 (1979).
12) Richardson, D. R. and Baker, E. Two saturable mechanisms of iron uptake from transferrin in human melanoma cells: the effect of transferrin concentration, chelators, and metabolic probes on transferrin and iron uptake. *J. Cell. Physiol.*, **161**, 160–168 (1994).
13) Kelm, S. and Schauer, R. The galactose-recognizing system of rat peritoneal macrophages. *Biol. Chem. Hoppe Seyler*, **367**, 989–998 (1986).
14) Muir, E. M. and Bowyer, D. E. Dependence of fluid-phase pinocytosis in arterial smooth muscle cells on temperature, cellular ATP concentration and cytoskeletal system. *Biochem. J.*, **216**, 467–473 (1983).
15) Roberts, W. G. and Berns, M. W. *In vitro* photosensitization I. Cellular uptake and subcellular localization of mono-L-aspartyl chlorin e6, chloro-aluminum sulfonated phthalocyanine, and photofrin II. *Lasers Surg. Med.*, **9**, 90–101 (1989).
16) Lin, C.-W., Shulok, J. R., Kirley, S. D., Cincotta, L. and Foley, J. W. Lysosomal localization and mechanism of uptake of nile blue photosensitizers in tumor cells. *Cancer Res.*, **51**, 2710–2719 (1991).
17) Kessel, D. Determinants of photosensitization by mono L-aspartyl chlorin e6. *Photochem. Photobiol.*, **49**, 447–452 (1989).
18) Nakajima, S., Takemura, T. and Sakata, I. Tumor-localizing activity of porphyrin and its affinity to LDL, transferrin. *Cancer Lett.*, **92**, 113–118 (1995).
19) Vitols, S., Angelin, B., Ericksson, S., Gahrton, G., Juliusson, G., Masquelier, M., Paule, C., Peterson, C., Rudling, C., Söderbery-Reid, K. and Tidefelt, U. Uptake of low density lipoproteins by human leukemic cells *in vivo*: relation to plasma lipoprotein levels and possible relevance for selective chemotherapy. *Proc. Natl. Acad. Sci. USA*, **87**, 2598–2602 (1990).
20) Gal, D., McDonald, P. C., Porter, J. C. and Simpson, E. R. Cholesterol metabolism in cancer cells in monolayer culture. III. Low-density lipoprotein metabolism. *Int. J. Cancer*, **28**, 315–319 (1981).
21) Norata, G., Canti, G., Ricci, L., Nicolin, A., Trezzi, E. and Catapano, A. L. *In vivo* assimilation of low density lipoprotein by a fibrosarcoma tumor line in mice. *Cancer Lett.*, **25**, 203–208 (1984).
22) Tajiri, H., Yokoyama, K., Boku, N., Ohtsu, A., Fujii, T., Yoshida, S., Sato, T., Hakamata, K., Hayashi, K. and Sakata, I. Fluorescent diagnosis of experimental gastric cancer using a tumor-localizing photosensitizer. *Cancer Lett.*, **111**, 215–220 (1997).
23) Roberts, W. G., Liaw, L.-H. L. and Berns, M. W. *In vitro* photosensitization I. An electron microscopy study of cellular destruction with mono-L-aspartyl chlorin e6 and photofrin II. *Lasers Surg. Med.*, **9**, 102–108 (1989).